JOURNAL OF VIROLOGY, July 2011, p. 7449–7453 Vol. 85, No. 14
0022-538X/11/$12.00 doi:10.1128/JVI.00255-11

Structure and Genetic Analysis of the Arterivirus Nonstructural Protein 7α▽#

Ioannis Manolaridis,[1]†¶ Cyril Gaudin,[2]‡¶ Clara C. Posthuma,[3]¶ Jessika C. Zevenhoven-Dobbe,[3] Isabelle Imbert,[4] Bruno Canard,[4] Geoff Kelly,[5] Paul A. Tucker,[1]¶ Maria R. Conte,[2]¶* and Eric J. Snijder[3]¶*

European Molecular Biology Laboratory, Hamburg Outstation, D-22603 Hamburg, Germany[1]; Randall Division of Cell and Molecular Biophysics, King's College London, New Hunt's House, Guy's Campus, London SE1 1UL, United Kingdom[2]; Molecular Virology Laboratory, Department of Medical Microbiology, Center of Infectious Diseases, Leiden University Medical Center, 2300 RC Leiden, the Netherlands[3]; Architecture et Fonction des Macromolecules Biologiques, CNRS and Universités d'Aix-Marseille I et II, UMR 6098, ESIL Case 925, Marseille, France[4]; and Biomedical NMR Centre, National Institute for Medical Research, Mill Hill, London NW7 1AA, United Kingdom[5]

Received 3 February 2011/Accepted 1 May 2011

Arterivirus replicase polyproteins are cleaved into at least 13 mature nonstructural proteins (nsps), and in particular the nsp5-to-nsp8 region is subject to a complex processing cascade. The function of the largest subunit from this region, nsp7, which is further cleaved into nsp7α and nsp7β, is unknown. Using nuclear magnetic resonance (NMR) spectroscopy, we determined the solution structure of nsp7α of equine arteritis virus, revealing an interesting unique fold for this protein but thereby providing little clue to its possible functions. Nevertheless, structure-based reverse genetics studies established the importance of nsp7/nsp7α for viral RNA synthesis, thus providing a basis for future studies.

Arteriviruses are enveloped viruses with an ~13- to ~16-kb plus-stranded RNA genome (17, 18). In general, the consequences of arterivirus infection can range from an asymptomatic, persistent, or acute infection to abortion or lethal hemorrhagic fever (11). The family currently comprises four members: equine arteritis virus (EAV) (1), lactate dehydrogenase-elevating virus (LDV) of mice, simian hemorrhagic fever virus (SHFV), and porcine reproductive and respiratory syndrome virus (PRRSV). The latter arterivirus has become an economically important pathogen, recently causing major outbreaks in the Asian swine industry (25).

Together with the distantly related families *Coronaviridae* and *Roniviridae*, the *Arteriviridae* belong to the order *Nidovirales* (7, 17). Despite major differences in virion size and morphology, as well as pathogenesis, the evolutionary relationship among nidoviruses is evident in particular from the organization and composition of the large replicase gene (4). This gene consists of the two 5′-most open reading frames (ORFs) of the genome—ORF1a and ORF1b, which are followed by a variable number of downstream ORFs encoding structural and accessory proteins.

Translation of the 5′-capped and 3′-polyadenylated arterivirus genome results in two large precursor polyproteins, pp1a and the C-terminally extended frameshift product pp1ab. These are cleaved by up to four virus-encoded proteases to yield at least 13 nonstructural proteins (nsps) (nsp1 to nsp12, including nsp7α and 7β) plus a substantial number of processing intermediates of unknown function (5, 19, 20, 21, 23, 26). Together, the nsps direct the formation of a membrane-anchored replication/transcription complex (RTC) that mediates both viral genome replication and the synthesis of a 3′-coterminal nested set of subgenomic (sg) mRNAs, a nidovirus hallmark (13, 15).

The replicase of the arterivirus prototype EAV encodes pp1a and pp1ab products of 1,727 and 3,175 amino acids (aa), respectively, which are processed by three ORF1a-encoded proteinases residing in nsp1, nsp2, and nsp4 (5, 26). Other important functional domains include three proposed transmembrane proteins (nsp2, nsp3, and nsp5), key enzymes for RNA synthesis, such as the RNA-dependent RNA polymerase (RdRp; nsp9) (1) and helicase (nsp10) (16), and a uridylate-specific endoribonuclease (NendoU; nsp11) (12) of unknown function.

Despite recent progress in arterivirus replicase dissection, various uncharacterized domains and nsps remain, including in particular the nsp5-to-nsp8 region (nsp5-8), which is extensively processed via alternative proteolytic cascades (23) and yields at least seven long-lived processing intermediates. The largest subunit in this region is nsp7 (225 aa in EAV), which is flanked by two small nsps (nsp6 and nsp8, of only 22 and 50 aa,

* Corresponding author. Mailing address for Eric J. Snijder: Molecular Virology Laboratory, Department of Medical Microbiology, Center of Infectious Diseases, Leiden University Medical Center, P.O. Box 9600, 2300 RC Leiden, the Netherlands. Phone: 31 71 526 1657. Fax: 31 71 526 6761. E-mail: e.j.snijder@lumc.nl. Mailing address for Maria R. Conte: Randall Division of Cell and Molecular Biophysics, King's College London, New Hunt's House, Guy's Campus, London SE1 1UL, United Kingdom. Phone: 44 207 8486194. Fax: 44 207 8486435. E-mail: sasi.conte@kcl.ac.uk.

¶ These authors contributed equally to this work.

† Present address: The Institute of Cancer Research, Chester Beatty Laboratories, 237 Fulham Road, London SW3 6JB, United Kingdom.

‡ Present address: Institut Génomique Fonctionelle de Lyon, Ens de Lyon, Lyon Cedex 07, France.

Supplemental material for this article may be found at http://jvi.asm.org/.

▽ Published ahead of print on 11 May 2011.

TABLE 1. Summary of structural statistics for the EAV nsp7α structure

NMR restraint or other structural statistic	Value for nsp7α
Total distance restraints (inter-residue)	1,707
Short range (residue i to $i + j$, $j = 1$)	644
Medium range (residue i to $I + j$, $2 \leq j \leq 4$)	437
Long range (residue i to $i + j$, $j > 4$)	626
Hydrogen bonds	32
Total dihedral angle restraints	100
ϕ	50
ψ	50
Restraint violations	
Distance restraint violation > 0.2 Å	None
Dihedral restraint violation > 5°	None
Average rmsd (Å) among the 20 refined structures	
Residues	11–122
Backbone of structured regions[a]	0.505
Heavy atoms of structured regions	1.230
Ramachandran statistics of 20 structures (% residues)	
Most favored regions	78.4
Additional allowed regions	19.3
Generously allowed regions	0.8
Disallowed regions	1.5

[a] Residues selected on the basis of ^{15}N backbone dynamics (residues 11 to 122).

respectively) that may modulate its function, whereas nsp5-8 and nsp5-7 likely constitute membrane-associated forms of nsp6-8 and nsp6-7. nsp7 was recently found to be internally cleaved by the nsp4 protease, yielding small amounts of nsp7α and nsp7β (20). Mutagenesis of the nsp7α/7β site suggested that it is critical for EAV replication, although the function of nsp7 remains unknown, and no homolog of the protein appears to be present in other RNA virus families.

In order to further our understanding of the role of arterivirus nsp7, we have now determined the solution structure of the 123-aa nsp7α, which is far more conserved among arteriviruses than nsp7β. The protein was found to have a unique fold and possesses no recognizable functional motifs. Subsequently, residues suggested to be functionally important by sequence comparison and the derived structure were probed by reverse genetics, yielding a variety of crippled and nonviable EAV mutants that underscore the relevance of nsp7/nsp7α for arterivirus biology.

EAV nsp7α is comprised of amino acid residues Gly1453 to Glu1575 of the pp1a replicase protein (EAV Bucyrus isolate), which are renumbered 1 to 123 hereafter for convenience. Recombinant nsp7α was expressed in *Escherichia coli* as described previously (6; see also the supplemental material), and its structure was determined by nuclear magnetic resonance (NMR) spectroscopy using standard protocols executed with the Crystallography and NMR System (CNS) software (2) (Table 1) as previously described (3). The 20 lowest-energy structures were superimposed using the backbone coordinates for residues 11 to 122 (Fig. 1A), giving an overall root mean square deviation (rmsd) between the family and the mean coordinate position of 0.505 Å for backbone atoms. The structural statistics for the family of 20 structures are reported in Table 1. The structural quality was assessed in terms of restraints violation (analyzed within CNS) and deviation from the ideal geometry (using the program PROCHECK-NMR) (Table 1).

The overall fold of nsp7α consists of a bundle of three α-helices packed against a mixed β-sheet formed by 4 antiparallel strands (β_2 to β_5) and one short parallel strand (β_1) arranged in a $\beta_1\beta_2\beta_5\beta_4\beta_3$ topology (Fig. 1B). The secondary-structure elements are as follows: α_1 (Asp11 to Leu21), β_1 (Ala25 to Ser28), α_2 (Ser38 toVal54), α_3 (Ala58 to Asp70), β_2 (Asp81to Ile86), β_3 (Ala93 to Lys96), β_4 (Leu99 to Lys107), and β_5 (Cys114 to Lys121). The two central strands, β_5 and β_4, are particularly long and twist around each other to form a central backbone onto which the other strands bolt.

nsp7α has four distinct hydrophobic regions essential for the correct folding of the protein (Fig. 1C). Most of the hydropho-

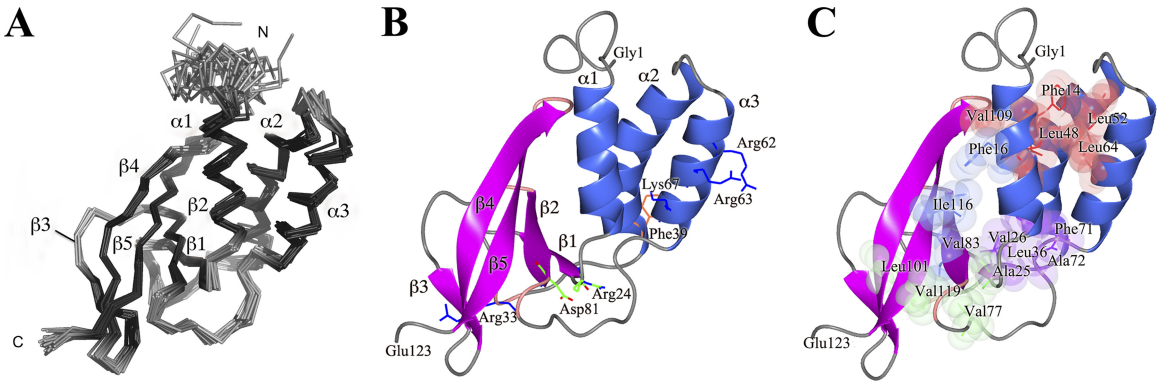

FIG. 1. The NMR structure of EAV nsp7α. (A) Cα trace of the 20 lowest-energy nsp7α solution structures superimposed for residues Asp11 to Glu122. (B) A cartoon representation in the same orientation as panel A. α-Helices are colored blue, β-strands magenta, and β-turns pink. The N and C termini are labeled, as are the surface residues referred to in the text discussing the mutagenesis results. The H-bonded residues Arg24 and Asp81 are shown in stick representation and colored according to atom type (C, green; N, blue; O, red). (C) A cartoon representation showing the hydrophobic residues that form the core of the fold. The residues are shown in stick representation and as semitransparent spheres with a radius equal to the van der Waals radius of the atoms. For clarity, the residues are divided by color into four hydrophobic patches, namely, red (Phe14, Leu17, Leu48, Leu52, Leu64, and Val109; Leu17 is fully obscured by Leu48 and was not labeled for clarity), magenta (Val26, Leu36, Ala72, and Phe71), blue (Phe16, Val83, and Ile116), and green (Ala25, Val77, Leu101, and Val119). Panels B and C were produced with ccp4mg (14).

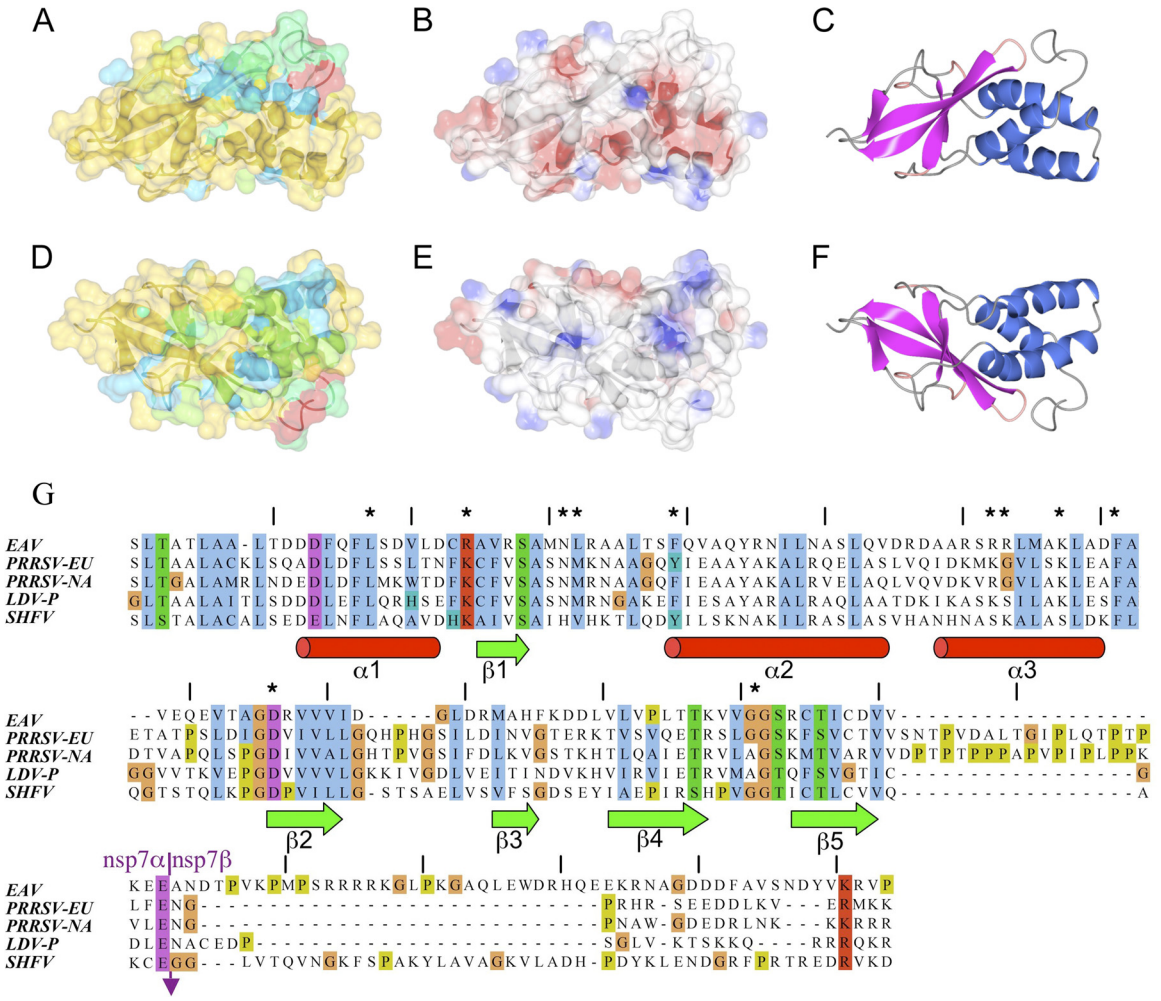

FIG. 2. Surface features, conservation, and mutagenesis of EAV nsp7α. Panels A to C are in the same orientation and are related to D to F by rotation of 180° about the horizontal axis. The semitransparent surfaces in panels A and D are colored according to sequence conservation, with red least conserved and blue most conserved. Panels B and E are colored according to electrostatic potential, with red corresponding to negative charge and blue to positive charge. For comparison, panels C and F are cartoon representations using the same coloring as in Fig. 1B. (G) Alignment of amino acid sequences of arterivirus nsp7α proteins, coupled with secondary-structure information from the EAV nsp7α three-dimensional structure. The alignment is based on sequence data for EAV (RefSeq no. NC_002532), European porcine respiratory and reproductive syndrome virus (PRRSV-EU; RefSeq no. M96262.2), North American porcine respiratory and reproductive syndrome virus (PRRSV-NA; RefSeq no. NC_001961), lactate dehydrogenase elevating virus strain Plagemann (LDV-P; RefSeq no. NC_001639), and simian hemorrhagic fever virus (SHFV; Refseq no. NC_003092). The alignment was produced with ClustalW2 (8) and edited with JalView. Residues are colored according to the standard ClustalW2 color scheme to indicate conservation. The (predicted) nsp7α/nsp7β cleavage site is indicated with an arrow, and the alignment of the region surrounding the nsp7α/nsp7β junction is based on a previously published sequence comparison (20). Asterisks indicate the EAV nsp7α residues that were probed by reverse genetics in this study (Leu17, Arg24, Asn31, Arg33, Phe39, Arg62, Arg63, Lys67, Phe71, Asp81, and Gly111). Panels A to F were produced with ccp4mg (14).

bic residues participating in the formation of those regions are either fully conserved among arteriviruses (Phe16, Leu17, Leu48, Leu52, Phe71, and Val83) or replaced by other hydrophobic residues (Phe14, Ala25, Val26, Leu36, Leu64, Ala72, Val77, Leu101, Val109, Ile116, and Val119), as shown in the sequence alignment presented in Fig. 2G.

Analysis of the nsp7α structure using EBI Web tools (PDBsum/ProFunc, Catalytic site search; http://www.ebi.ac.uk), Dali (http://ekhidna.biocenter.helsinki.fi/dali_server/), and GRATH (http://protein.hbu.cn/cath/cathwww.biochem.ucl.ac.uk/cgi-bin/cath/Grath.html) did not result in any significant indicators of function or similarities in structure. The structure, therefore, represents a new fold and provides little clue about potential functions of nsp7α. Furthermore, electrostatic surface potential analysis revealed a rather mixed set of surface charges, with no clear electropositive or electronegative patches that would point toward the nsp7α function. (Fig. 2B and E).

To assess the relationship between nsp7α and its precursor, nsp7, we performed a comparison of the amide group chemical shifts for the two proteins using NMR spectroscopy. The full-length nsp7 coding sequence (nucleotides [nt] 4583 to 5255, encoding pp1a/pp1ab residues Ser1453 to Glu1677; EAV Bucyrus isolate) was also expressed in *E. coli* and purified as described for nsp7α (see the supplemental material). Many of the resonances of nsp7α do not appear to change significantly

Residue	Mutant	wt codon	mutant codon	IFA 16 h pt	IFA 24 h pt	titer 16 h pt (PFU/ml)	titer 24 h pt (PFU/ml)	Summary of phenotype
Leu-1469	Leu17→Asp	CUC	GAC	negative	negative	ND	$< 10^1$	non-viable
Arg-1476	Arg24→Ala	CGG	GCG	positive	positive	7×10^5	6×10^6	crippled; small plaques
Arg-1485	Arg33→Ala	CGU	GCU	negative	few positive cells	ND	$< 10^1$	severely crippled; possible reversion
Phe -1491	Phe39→Ala	UUU	GCU	negative	negative	ND	$< 10^1$	non-viable
Arg-1514	Arg62→Ala	CGC	GCC	positive	positive	6×10^5	7×10^6	crippled, intermediate plaques
Arg-1515	Arg63→Ala	AGA	GCA	positive	positive	$< 10^1$	$< 10^1$	crippled; RNA synthesis, but no progeny
Lys-1519	Lys67→Ala	AAA	GCA	few positive cells	few positive cells	$< 10^1$	$< 10^1$	severely crippled; RNA synthesis, but no progeny
	Lys67→Arg	AAA	AGA	strongly positive	strongly positive	4×10^7	2×10^8	slightly crippled; intermediate plaques
	Lys67→Ser	AAA	AGU	few cells positive	few cells positive	$< 10^1$	2×10^3	severely crippled; pseudoreversion to Arg67
Phe-1523	Phe71→Asp	UUU	GAU	negative	negative	ND	$< 10^1$	non-viable
Asp-1533	Asp81→Ala	GAC	GCC	negative	negative	ND	4×10^3	severely crippled; reversion to wt
	Asp81→Asn	GAC	AAC	few cells positive	few cells positive	$< 10^1$	$< 10^1$	severely crippled; possible reversion
	Asp81→Glu	GAC	GAG	strongly positive	strongly positive	5×10^6	2×10^7	crippled; small plaques
Gly-1563	Gly111→Asp	GGU	GAU	barely positive	positive	small: 5×10^2 large: 1×10^2	small: 3×10^3 large: 1×10^3	crippled; mixed plaque sizes; reversion to wt
wt control	N.A.	N.A.	N.A.	strongly positive	strongly positive	4×10^8	5×10^8	wt virus control

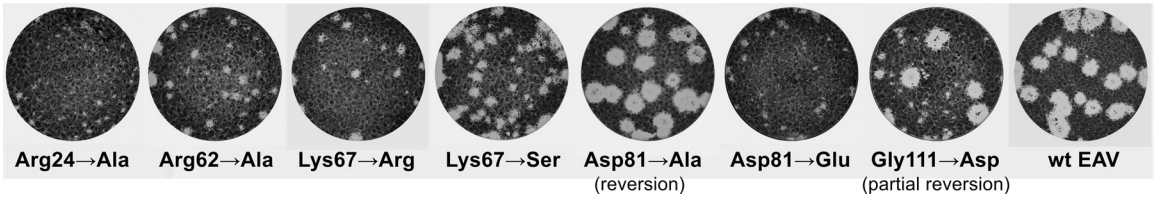

FIG. 3. Genotype and phenotype of EAV nsp7α mutants. The details of EAV nsp7α mutants engineered in this study are listed, and amino acid numbers for both the EAV pp1a/pp1ab replicase polyproteins and the 123-aa nsp7α protein described in this study are provided. BHK-21 cells transfected with synthetic full-length EAV RNA carrying these mutations were analyzed by immunofluorescence microscopy at 16 and 24 h posttransfection, and supernatants were harvested for plaque assays. Plaque assays were fixed and stained with crystal violet at 40 h postinfection, and images of a selection of mutants are shown in the lower part of the figure. wt, wild type.

in the context of the full-length nsp7 (see Fig. S1 in the supplemental material). Overall, our data indicate that the nsp7α core structure is also present in the full-length protein and that the nsp7α/7β cleavage is very unlikely to be accompanied by a large conformational change in the nsp7α core.

On the basis of the EAV nsp7α structure and an nsp7 sequence alignment (Fig. 2G), a number of conserved and less-conserved nsp7α residues were selected for site-directed mutagenesis and reverse genetics. Mutations were introduced into an EAV infectious cDNA clone and, after electroporation of *in vitro*-transcribed full-length RNA, the viability of the mutant viruses was analyzed using immunofluorescence assays for the viral replicase subunit nsp3 and the nucleocapsid (N) protein, which can be used as markers for the synthesis of genomic and sg mRNA7, respectively (22). Furthermore, cell culture supernatants were harvested and tested in a plaque assay for the production of infectious virus progeny (Fig. 3). Finally, the occurrence of reversion was monitored by virus passaging and sequence analysis.

Figure 3 summarizes the results of our mutagenesis study. The residues selected for mutagenesis either were thought to be important for protein folding, as deduced from the structure (Leu17, Arg24, Phe71, Asp81, and Gly111), or were residues with solvent-accessible side chains (Arg33, Phe39, Arg62, Arg63, and Lys67). Leu17 and Phe71 are buried within the hydrophobic cores presented above and are fully conserved among arteriviruses (Fig. 2G). Gly111 is conserved in the sense that the residue is small (either Gly or Ala), which is important for the stability of the β-turn between strands β4 and β5. Mutation of these residues to Asp might disrupt the core, and therefore, the protein fold, explaining the nonviable (Leu17→Asp and Phe71→Asp) and crippled (Gly111→Asp) phenotype of these mutants. Arg24 (in the loop between helices α_1 and α_2) and Asp81 (in β-strand β_1) form a salt bridge that keeps the α-helical bundle stacked against the β-sheet (Fig. 1B). Its disruption by replacement of Arg24 with Ala indeed crippled virus replication. A range of phenotypes was observed for substitutions of the fully conserved Asp81 residue. The drastic change to Ala led to a quasiviable phenotype that did not produce plaques upon analysis of early virus harvests but subsequently reverted to the wild-type residue, indicating that a low level of viral RNA synthesis must have been maintained by this mutant. The more conservative Asp81→Glu substitution resulted in a viable but crippled mutant.

Residues Arg33, Phe39, Arg62, Arg63, and Lys67 are ex-

posed on the protein surface and therefore could be of functional importance. In particular, the positively charged Arg33 (semiconserved), Arg62 (semiconserved), and Arg63 (not conserved) may provide suitable binding regions for the phosphate backbone of an oligonucleotide. Substitution of these residues resulted in crippled mutants, whereas replacement of Lys67 with another positively charged residue (i.e., Arg) had only a mild effect, strengthening our hypothesis. Interestingly, a replacement of Lys67 with Ser, the residue present at the corresponding position in SHFV nsp7α, pseudoreverted to Arg, suggesting that indeed a positively charged residue is preferred at position 67. For the Lys67→Ala mutant, some cells were positive in immunofluorescence assays but we repeatedly could not detect progeny virus. The solvent-accessible side chain of the (conserved aromatic) Phe39, which could provide stacking interactions with nucleotide bases, was found to be essential for virus viability.

In the complex proteolytic cascade used to mature the nsp3-8 region of the EAV pp1a and pp1ab replicase polyproteins, nsp7 (nsp7α) stands out for the number of long-lived processing intermediates that contain this subunit. The nsp4 cleavage sites involved in these proteolytic events are all conserved throughout the arterivirus group, suggesting that this multitude of nsp7-containing processing intermediates may be a common feature of arterivirus-infected cells (5, 20, 26). The structural analysis presented in this paper defines EAV nsp7α, the most conserved region of nsp7 (Fig. 2G), as a distinct replicase domain with a novel fold, a fold that is likely preserved in the C-terminally extended full-length nsp7. Even though the nsp7α structure and reverse genetics analysis provided us few clues about the (putative) function(s) of this protein, some valuable conclusions can be drawn, and we provide the first direct evidence that nsp7α indeed is a critical protein domain for arterivirus RNA synthesis (Fig. 3). Interpretation of the observed mutant phenotypes is complicated by their diversity and the fact, outlined above, that nsp7α is part of so many replicase-processing intermediates. As in other plus-stranded RNA virus systems, e.g., picornaviruses and alphaviruses (9, 10, 24), such intermediates may perform specific functions themselves and proteolytic cleavages may serve as a switch to (in)activate them. In any case, all replacements of nsp7α residues tested in this study affected some aspect of the EAV replicative cycle, indicating that they are structurally or functionally important and justifying the future in-depth characterization of these mutant phenotypes.

Protein structure accession number. Structure data for the arterivirus nsp7α are available in the Protein Data Bank under accession number 2L8K.

We thank our LUMC colleagues Nancy Beerens, Linda Boomaars-van der Zanden, and Ali Tas; Bruno Coutard (AFMB Marseille); and Luigi Martino (King's College London) for excellent technical assistance.

This work was supported in part by the European project "VIZIER" ("Comparative Structural Genomics of Viral Enzymes Involved in Replication") funded by the 6th Framework Programme of the European Commission under the reference LSHG-CT-2004-511960, and by NWO-CW TOP grant 700.57.301 from the Netherlands Organization for Scientific Research. M. R. Conte is indebted to the Wellcome Trust for financial support.

REFERENCES

1. **Beerens, N., et al.** 2007. De novo initiation of RNA synthesis by the arterivirus RNA-dependent RNA polymerase. J. Virol. **81:**8384–8395.
2. **Brünger, A. T.** 2007. Version 1.2 of the crystallography and NMR system. Nat. Protoc. **2:**2728–2733.
3. **Conte, M. R., et al.** 2006. Structure of the eukaryotic initiation factor (eIF) 5 reveals a fold common to several translation factors. Biochemistry **45:**4550–4558.
4. **den Boon, J. A., et al.** 1991. Equine arteritis virus is not a togavirus but belongs to the coronaviruslike superfamily. J. Virol. **65:**2910–2920.
5. **Fang, Y., and E. J. Snijder.** 2010. The PRRSV replicase: exploring the multifunctionality of an intriguing set of nonstructural proteins. Virus Res. **154:**61–76.
6. **Gaudin, C., I. Manolaridis, P. A. Tucker, and M. R. Conte.** 2010. Resonance assignment of nsp7alpha from arterivirus. Biomol. NMR Assign. **5:**23–25.
7. **Gorbalenya, A. E., L. Enjuanes, J. Ziebuhr, and E. J. Snijder.** 2006. Nidovirales: evolving the largest RNA virus genome. Virus Res. **117:**17–37.
8. **Larkin, M. A., et al.** 2007. Clustal W and Clustal X version 2.0. Bioinformatics **23:**2947–2948.
9. **Lawson, M. A., and B. L. Semler.** 1992. Alternate poliovirus nonstructural protein processing cascades generated by primary sites of 3C proteinase cleavage. Virology **191:**309–320.
10. **Lemm, J. A., T. Rumenapf, E. G. Strauss, J. H. Strauss, and C. M. Rice.** 1994. Polypeptide requirements for assembly of functional Sindbis virus replication complexes: a model for the temporal regulation of minus- and plus-strand RNA synthesis. EMBO J. **13:**2925–2934.
11. **Maclachlan, N. J., U. B. Balasuriya, M. P. Murtaugh, S. W. Barthold, and L. J. Lowenstine.** 2007. Arterivirus pathogenesis and immune response, p. 325–337. *In* S. Perlman, T. Gallagher, and E. J. Snijder (ed.), Nidoviruses. ASM Press, Washington, DC.
12. **Nedialkova, D. D., et al.** 2009. Biochemical characterization of arterivirus nonstructural protein 11 reveals the nidovirus-wide conservation of a replicative endoribonuclease. J. Virol. **83:**5671–5682.
13. **Pasternak, A. O., W. J. M. Spaan, and E. J. Snijder.** 2006. Nidovirus transcription: how to make sense.? J. Gen. Virol. **87:**1403–1421.
14. **Potterton, E., S. McNicholas, E. Krissinel, K. Cowtan, and M. Noble.** 2002. The CCP4 molecular-graphics project. Acta Crystallogr. **58:**1955–1957.
15. **Sawicki, S. G., D. L. Sawicki, and S. G. Siddell.** 2007. A contemporary view of coronavirus transcription. J. Virol. **81:**20–29.
16. **Seybert, A., L. C. van Dinten, E. J. Snijder, and J. Ziebuhr.** 2000. Biochemical characterization of the equine arteritis virus helicase suggests a close functional relationship between arterivirus and coronavirus helicases. J. Virol. **74:**9586–9593.
17. **Snijder, E. J., and J. J. M. Meulenberg.** 1998. The molecular biology of arteriviruses. J. Gen. Virol. **79:**961–979.
18. **Snijder, E. J., and W. J. M. Spaan.** 2006. Arteriviruses, p. 1337–1355. *In* D. M. Knipe and P. M. Howley (ed.), Fields virology. Lippincott, Williams & Wilkins, Philadelphia, PA.
19. **van Aken, D., E. J. Snijder, and A. E. Gorbalenya.** 2006. Mutagenesis analysis of the nsp4 main proteinase reveals determinants of arterivirus replicase polyprotein autoprocessing. J. Virol. **80:**3428–3437.
20. **van Aken, D., J. C. Zevenhoven-Dobbe, A. E. Gorbalenya, and E. J. Snijder.** 2006. Proteolytic maturation of replicase polyprotein pp1a by the nsp4 main proteinase is essential for equine arteritis virus replication and includes internal cleavage of nsp7. J. Gen. Virol. **87:**3473–3482.
21. **van Dinten, L. C., S. Rensen, W. J. M. Spaan, A. E. Gorbalenya, and E. J. Snijder.** 1999. Proteolytic processing of the open reading frame 1b-encoded part of arterivirus replicase is mediated by nsp4 serine protease and is essential for virus replication. J. Virol. **73:**2027–2037.
22. **van Dinten, L. C., H. van Tol, A. E. Gorbalenya, and E. J. Snijder.** 2000. The predicted metal-binding region of the arterivirus helicase protein is involved in subgenomic mRNA synthesis, genome replication, and virion biogenesis. J. Virol. **74:**5213–5223.
23. **Wassenaar, A. L. M., W. J. M. Spaan, A. E. Gorbalenya, and E. J. Snijder.** 1997. Alternative proteolytic processing of the arterivirus replicase ORF1a polyprotein: evidence that NSP2 acts as a cofactor for the NSP4 serine protease. J. Virol. **71:**9313–9322.
24. **Ypma-Wong, M. F., D. J. Filman, J. M. Hogle, and B. L. Semler.** 1988. Structural domains of the poliovirus polyprotein are major determinants for proteolytic cleavage at Gln-Gly pairs. J. Biol. Chem. **263:**17846–17856.
25. **Zhou, L., and H. Yang.** 2010. Porcine reproductive and respiratory syndrome in China. Virus Res. **154:**31–37.
26. **Ziebuhr, J., E. J. Snijder, and A. E. Gorbalenya.** 2000. Virus-encoded proteinases and proteolytic processing in the *Nidovirales*. J. Gen. Virol. **81:**853–879.